# Quaternary Structure of $V_1$ and $F_1$ ATPase: Significance of Structural Homologies and Diversities[†]

Dmitri I. Svergun,[‡,§] Stephanie Konrad,[ǁ] Markus Huss,[⊥] Michel H. J. Koch,[‡] Helmut Wieczorek,[⊥]
Karlheinz Altendorf ,[ǁ] Vladimir V. Volkov,[§] and Gerhard Grüber*[,ǁ]

*European Molecular Biology Laboratory, Hamburg Outstation, Notkestrasse 85, D-22603 Hamburg, Germany, Institute of
Crystallography, Russian Academy of Sciences, Leninsky pr. 59, 117333 Moscow, Russia, and Universität Osnabrück,
Fachbereich Biologie/Chemie, Abteilung Mikrobiologie and Abteilung Zoophysiologie, D-49069, Osnabrück, Germany*

ABSTRACT: The $V_1$ ATPase from the tobacco hornworm *Manduca sexta* and the *Escherichia coli* $F_1$ ATPase
were characterized by small-angle X-ray scattering (SAXS). The radii of gyration ($R_g$) of the complexes
were $6.2 \pm 0.1$ and $4.7 \pm 0.02$ nm, respectively. The shape of the *M. sexta* $V_1$ ATPase was determined
ab initio from the scattering data showing six masses, presumed to be the A and B subunits, arranged in
an alternating manner about a 3-fold axis. A seventh mass with a length of about 11.0 nm extends
perpendicularly to the center of the hexameric unit. This central mass is presumed to be the stalk that
connects $V_1$ with the membrane domain ($V_O$) in the intact $V_1V_O$-ATPase. In comparison, the shape of the
$F_1$ ATPase from *E. coli* possesses a quasi-3-fold symmetry over the major part of the enzyme. The overall
asymmetry of the structure is given by a stem, assumed to include the central stalk subunits. The features
of the $V_1$ and $F_1$ ATPase reveal structural homologies and diversities of the key components of the
complexes.

Some biomolecular assemblies consist of a mosaic of globular structural units including domain or supersecondary structures. These structural units also serve as functional units that play specific roles in the activity. V- and F-ATPases represent clear examples of mosaic structures. They belong to a class of pumps that couple synthesis or hydrolysis of ATP to the translocation of $H^+$ or $Na^+$ across the membrane. Each enzyme consists of a peripheral part, $V_1$ or $F_1$, that contains the catalytic sites and a membrane-bound part, $V_O$ or $F_O$, that conducts the ion flow (*1−3*). The two major catalytic subunits in the $V_1$ ATPase (*A* and *B*) with a stoichiometry of $A_3B_3$ and in the $F_1$ ATPase ($\alpha_3\beta_3$) have more than 25% primary sequence similarity, whereas it is difficult to identify $V_1$ subunits that would have any similarity to the smaller polypeptides of $F_1$ even though the sequences of most of these subunits have been determined (*4, 5*).

The smaller $V_1$ subunits C, D, E, F, and G are described as "stalk" subunits (*6*) and appear to bridge the $V_1$ and $V_O$ parts as seen in electron microscopy images of V ATPase-containing membranes (*7, 8*). More structural information is available on the F-ATPases. The recently determined high-resolution structures of the $\alpha_3\beta_3\gamma$ subcomplex of the beef heart mitochondria (*9*) and rat liver mitochondria $F_1$ part (*10*) provide a picture in which the three $\alpha$ and $\beta$ subunits are arranged in a hexagon around a part of subunit $\gamma$. The latter extends from the bottom of $F_1$ into a stalk that separates the $F_1$ and membrane-embedded $F_O$ parts. Unfortunately, in the two crystal forms of $F_1$, the smaller $F_1$ subunits $\delta$ and $\epsilon$ are disordered (*9, 10*).

Here, we report for the first time structural studies of the $V_1$ ATPase from the tobacco hornworm *Manduca sexta* in solution using small-angle X-ray scattering (SAXS).[1] The overall structure of the $V_1$ ATPase allows a comparison with the shape of the *Escherichia coli* $F_1$ ATPase determined in close to physiological conditions.

## EXPERIMENTAL PROCEDURES

*Scattering Experiments and Data Analysis.* The synchrotron radiation X-ray scattering data were collected on the X33 camera (*11−13*) of the European Molecular Biology Laboratory (EMBL) on the storage ring DORIS III of the Deutsches Elektronen Synchrotron (DESY) using multiwire proportional chambers with delay line readout (*14*). At the sample−detector distance of 3.8 m and the wavelength $\lambda = 0.15$ nm the range of momentum transfer $0.14$ nm$^{-1} < s < 2.1$ nm$^{-1}$ was covered ($s$ is the modulus of the momentum transfer $s$, $s = 4\pi \sin \theta/\lambda$ where $2\theta$ is the scattering angle). The data were normalized to the intensity of the incident beam and corrected for the detector response, the scattering

* To whom correspondence should be addressed: Dr. Gerhard Grüber, Universität Osnabrück, Fachbereich Biologie/Chemie, D-49069 Osnabrück, Germany. Phone: +49/(0)541 969 2809. Fax: +49/(0)-541 969 2870. E-mail: grueber@biologie.uni-osnabrueck.de.

‡ EMBL-Outstation Hamburg.
§ Institute of Crystallography, Russian Academy of Sciences.
ǁ Abteilung Mikrobiologie, Universität Osnabrück.
⊥ Abteilung Zoophysiologie, Universität Osnabrück.

[1] Abbreviations: SAXS, small-angle X-ray scattering; SDS, sodium dodecyl sulfate.

of the buffer was subtracted, and the difference curves were scaled for concentration using the program SAPOKO (Svergun & Koch, unpublished results).

The maximum dimensions $D_{max}$ of the $V_1$ and $F_1$ ATPase were estimated from the experimental curves using the orthogonal expansion program *ORTOGNOM* (*15*). The distance distribution functions $p(r)$ and the radii of gyration $R_g$ were evaluated by the indirect Fourier transform program *GNOM* (*16, 17*). The Porod volumes $V_p$ were calculated from the processed (backtransformed from the $p(r)$) scattering curves as described by Feigin and Svergun (*18*), Ch. 3.3.3.

The low-resolution particle envelopes were restored from the experimental data using the ab initio shape determination procedure of Svergun and Stuhrmann (*19*) and Svergun et al. (*20, 21*). The particle shape is represented by an angular envelope function $r = F(\omega)$ where $(r,\omega)$ are spherical coordinates. The envelope is parametrized as

$$F(\omega) = \sum_{l=0}^{L} \sum_{m=-l}^{l} f_{lm} Y_{lm}(\omega) \tag{1}$$

where $Y_{lm}(\omega)$ are spherical harmonics and the multipole coefficients $f_{lm}$ are complex numbers. Series (1) contains in the general case $M = (L + 1)^2$ parameters and provides a spatial resolution of approximately $\delta r = \sqrt{5}\pi R_g/[\sqrt{3}(L + 1)]$. The scattering intensity of the envelope is evaluated as (*22*)

$$I(s) = 2\pi^2 \sum_{l=0}^{\infty} \sum_{m=-l}^{l} |A_{lm}(s)|^2 \tag{2}$$

where the partial amplitudes $A_{lm}(s)$ are calculated from the coefficients $f_{lm}$ using the recurrence relation of ref *19*. These coefficients can be determined by minimizing the discrepancy between the calculated and the experimental curves

$$R_I^2 = \frac{\sum\limits_{j=1}^{N} \{W(s_j)[I(s_j) - I_{exp}(s_j)]\}^2}{\sum\limits_{j=1}^{N} [W(s_j)I_{exp}(s_j)]^2} \tag{3}$$

where $N$ is a number of experimental points and the weighting function is $W(s_j) = s_j^2/[\sigma(s_j)/I_{exp}(s_j)]$, where $I_{exp}(s_j)$ and $\sigma(s_j)$ are the experimental intensity and its standard deviation in the $j$-th point, respectively.

The major parts of the molecules of $V_1$ and $F_1$ ATPase are known to possess quasi-3-fold symmetry (*7, 23*). This symmetry restriction leads to selection rules for the coefficients $f_{lm}$ and was employed to reduce the number of parameters in series 1. Thus, at a resolution of $L = 5$ the description of a symmetric envelope using series 1 requires $M = 12$ parameters instead of $M = 36$ for the general case. The shape determination was performed assuming a 3-fold symmetry by the minimization program *SASHA* (*20, 21*). The program starts from a spherical initial approximation and fits the experimental data by a nonlinear optimization procedure with additional penalties to keep the particle surface smooth and its envelope function positive definite.

*Other Methods.* Purification of the $V_1$ ATPase from *M. sexta*, protein determination with Amido Black, standard



FIGURE 1: $V_1$ ATPase purified from starving *Manduca sexta* larvae. $V_1$ ATPase (1 $\mu$g) was applied to an SDS−polyacrylamide gel, and the subunits were stained with silver.

SDS−polyacrylamide gel electrophoresis, and ATPase activity measurements were performed as described previously (*24, 25*). The purification of *E. coli* $F_1$ ATPase was accomplished according to Grüber et al. (*26*). The protein concentration of $F_1$ was determined according to Dulley and Grieve (*27*), and ATP hydrolysis was measured as described by Fiske and Subbarow (*28*) and Arnold et al. (*29*).

## RESULTS AND DISCUSSION

For the experiments described here the $V_1$ ATPase of the larval *M. sexta* midgut was isolated to homogeneity (*24*). Figure 1 presents an SDS-polyacrylamide gel (17.5% total and 0.4% cross-linked acrylamide) of the $V_1$ ATPase used in the small-angle X-ray studies. The enzyme contains the seven subunits A, B, C, D, E, F, and G. At first glance, subunit C appears to be present in substoichiometric amounts. However, as our data will show, the $V_1$ complex is homogeneous; moreover, as shown previously, the intensity of subunit C in silver-stained SDS−polyacrylamide gels is weak in comparison to gels stained with Coomassie blue (*30, 31*). So far there is no unequivocal indication for the presence of subunit H which is a constituent member of the catalytic $V_1$ complex in yeast (Vma13p (*32*)) and in bovine clathrin-coated vesicles (SFD (*33*)). The ATP hydrolysis rates as isolated were 1.9 $\mu$mol of ATP hydrolyzed per milligram of protein per minute in the presence of 25% methanol. Figure 2 shows the experimental solution X-ray scattering profile of 10 mg of $V_1$ ATPase per mL. The asymmetric profile of the distance distribution function $p(r)$ is characterized by the radius of gyration, $R_g = 6.2 \pm 0.1$ nm, peak position at 6.7 $\pm$ 0.3 nm and the maximum particle dimension, $D_{max}$, at 22.0 $\pm$ 0.1 nm (see Figure 3). This indicates that, in the present solvent condition, the structure of the $V_1$ ATPase is rather elongated. Comparison of the normalized forward scattering with the values obtained for a reference solution of bovine serum albumin yields a molecular mass of 550 $\pm$ 20 kDa, in agreement with a molar ratio of $A_3:B_3:C:D:E:F:G_3$ and apparent molecular masses of 67, 56, 40, 32, 28, 14, and 16 kDa. These indicate that aggregation of the enzyme complex does not occur at the concentrations used. The Porod volume of $V_1$ is 970 $\pm$ 30 nm$^3$, and this is in good agreement with the molecular mass estimation. The hydrolytic activity of the $V_1$ ATPase after exposure to X-rays was 2.2 $\mu$mol of ATP hydrolyzed per milligram per minute, indicating that the enzyme was not damaged by X-rays.

The low-resolution envelope of $V_1$ was determined ab initio from the experimental data as described in Materials and Methods assuming a 3-fold symmetry. The maximum
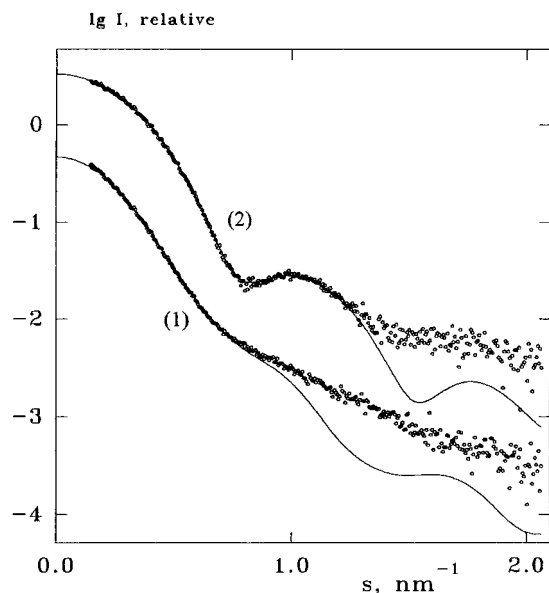
FIGURE 2: Experimental and calculated curves of the $V_1$ (1) and $F_1$ ATPase (2): dots, experimental data; solid lines, scattering from the restored envelopes in Figure 3. The $V_1$ curves are displaced down one logarithmic unit for clarity. The $V_1$ ATPase (10 mg/mL) was dissolved in 20 mM Tris-MOPS (pH 8.1) and 30 mM NaCl. The X-ray scattering of the *E. coli* $F_1$ ATPase (10 mg/mL) was measured after incubation (10 min) with 2 mM MgATP (ratio of 1:1) at room temperature.
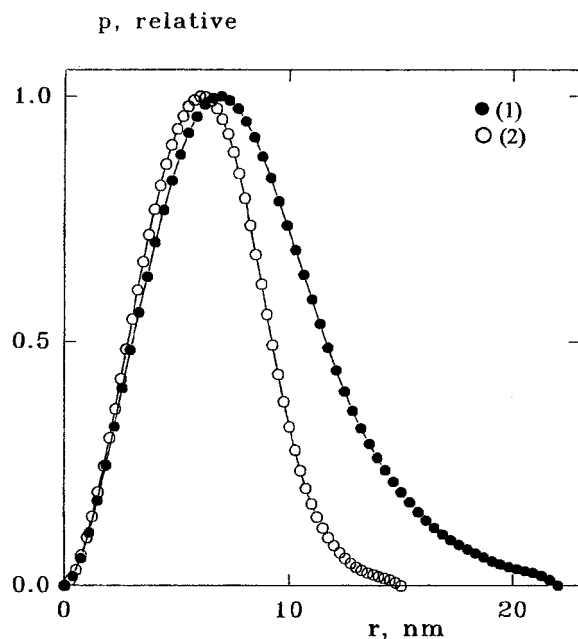


FIGURE 3: Distance distribution functions of $V_1$ (1) and $F_1$ ATPase (2) evaluated by the program *GNOM*. The functions are normalized to a maximum value of unity for better visualization.

order of harmonics $L$ in series 1 was chosen to keep the number of free parameters $M$ close to the number of Shannon channels in the experimental data $N_s = s_{max}D_{max}/\pi$. As shown by Svergun et al. (*20*), shape determination is unique when $M$ does not exceed $1.5N_s$. The value of $N_s$ was 14.4 allowing the use of $L = 6$ ($M = 17$) for the restoration. The restored envelope of $V_1$ (spatial resolution 3.6 nm) is presented in Figure 4. The final agreement to the experimental data is displayed in Figure 2, yielding a $R_I$ value of $2.5 \times 10^{-2}$. The $R_I$ values were evaluated using eq 3 in the entire range. Note that, as the scattering curves decrease rapidly with $s$,
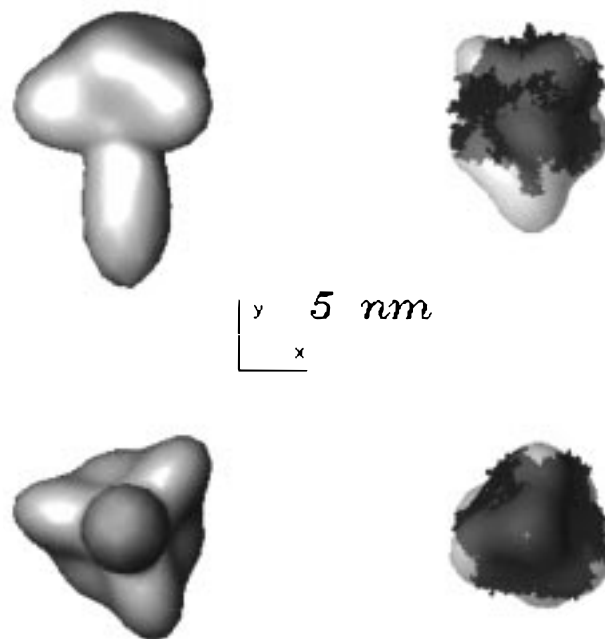


FIGURE 4: Low-resolution envelopes of ATPases: $V_1$ complex (left panel) and $F_1$ complex (right panel). The atomic model of the beef heart mitochondria $\alpha_3\beta_3$ subassembly ($\alpha_{DP}19-510$, $\alpha_{TP}25-510$, $\alpha_E24-510$, and $\beta9-474$) and the part of subunit $\gamma$ ($\gamma1-45$, $\gamma73-90$, and $\gamma209-272$ (*9*)) are positioned inside the low-resolution model of the *E. coli* $F_1$ ATPase (right panel): bottom images, view along the 3-fold axis (Z); top images are rotated counterclockwise around the $X$ axis by 90°. The models were displayed on a SUN Workstation using the program *ASSA* (*48*).

the discrepancies in the outer part of the curve contribute less to the entire $R$ factor. The form of the $R$ factor (3) was found to be optimal for low-resolution shape restoration in earlier studies (*34*). The outer part of the scattering curve cannot be fitted neatly, because of the increasing contribution from the scattering due to the internal inhomogeneities at higher angles, and also because of the resolution limitations of the spherical harmonics representation of highly anisometric shapes. However, the deviation at higher angles does not influence the following conclusions about the gross features of the particle shape as those are defined by the initial part of the curve ($s < 1$ nm$^{-1}$).

The envelope of $V_1$ ATPase is rather elongated with a globular structure at the top consisting essentially of six masses, assumed to be the subunits A and B, arranged in an alternating manner (see Figure 4). An elongated, symmetrical "stalk" with a length of about 11.0 nm runs perpendicularly to that hexameric mass. These structural features are also those found in images of negatively stained single particles of this $V_1$ complex showing six major masses of density in a pseudohexagonal arrangement surrounding a central seventh mass (Rademacher, Ruiz, Wieczorek, and Grüber, unpublished data). A stalk of the dimensions shown in Figure 4 could accommodate the mostly $\alpha$-helical and elongated subunits C, D, E, F, and G (*35–39*) with a total molecular mass of about 162 kDa, assuming a stoichiometry of C:D: E:F:G$_3$. It should be noted that, in comparison to recent electron micrographs of negatively stained V-ATPase from *Clostridium fervidus* (*40*), the headpiece of the *M. sexta* $V_1$ complex exhibits a more rounded feature. Whether this difference is due to negative staining cannot be decided at present; studies applying cryoelectron microscopic techniques

which help to preserve speciments of the enzyme in their native structure in a thin layer of amourphous ice may solve this problem. Correspondent studies are ongoing in our laboratoury.

Previously, we have characterized the $F_1$ ATPase (stoichiometry $\alpha_3\beta_3\gamma\delta\epsilon$) from *E. coli* by small-angle X-ray scattering in the presence of 10% glycerol, which prevented the interpretation of the scattering data at larger angles ($s \geq 1.5$ nm$^{-1}$) (*41*). As demonstrated in the scattering profile in Figure 2 the data could be improved ($0.1 \leq s$ (nm$^{-1}$) $\geq 2.0$) using buffer without glycerol, which allowed the comparison with the scattering profile of the $V_1$ ATPase described above. The $R_g$ and $D_{max}$ for the $F_1$ complex have values of $4.7 \pm 0.02$ and $15.0 \pm 0.5$ nm, respectively. The Porod volume of $F_1$ is $640 \pm 20$ nm$^3$, in agreement with the molecular mass estimate of $390 \pm 20$ kDa. The profile of the $p(r)$ function has a peak at $6.1 \pm 0.2$ nm, and a $F_1$ molecule thus appears more compact than the $V_1$ one.

The shape of $F_1$ ATPase at a resolution of 3.2 nm was evaluated ab initio from its solution scattering curve yielding $R_I = 9.3 \times 10^{-3}$, and a compact envelope function obtained is illustrated in Figure 4. The central part of the envelope has a pronounced 3-fold symmetry and can be identified as the $\alpha_3\beta_3$ subcomplex as described recently ((*41*); see also Figure 4). The overall asymmetry of the structure is given by a short stem at the bottom of the molecule, assumed to include the central stalk subunits $\gamma$ and $\epsilon$, which are involved in the conformational coupling that links catalytic site events in the $\alpha_3\beta_3$ complex with ion pumping through the $F_O$ sector (*42*–*46*).

The structural parameters and the shape determination of $V_1$ and $F_1$ obtained from small-angle X-ray scattering give a well-defined description of the structural features of these complexes. The major differences in the quaternary structure of the two molecules are that the $V_1$ complex is not only larger but also more anisometric than the $F_1$ complex. The significant length of the stalk of $V_1$, which separates the catalytic part from the ion-conducting part, requires conformational coupling of the stalk subunits during ATP hydrolysis. This implies an enzymatic mechanism which postulates movement of stalk subunits or parts of them with respect to one another as well as to the peripheral A and B subunits. The key to understanding the mechanism of catalytic coupling is to characterize the structural changes in the $V_1$ complex during ATP hydrolysis. If they are sufficiently large, the conformational changes of macromolecular assemblies are better studied in solution to avoid the interference with the packing forces in the crystal on the changes, as already observed in other cases (*47*). Small-angle X-ray scattering combined with other techniques to study these conformational changes in the future should lead to a rational interpretation of the mechanism of conformational coupling.

## ACKNOWLEDGMENT

## REFERENCES

1. Stevens, T. H., and Forgac, M. (1997) *Annu. Rev. Cell Dev. Biol. 13*, 779–808.
2. Fillingame, R. H. (1997) *Curr. Opin. Struct. Biol. 6*, 491–498.
3. Dimroth, P. (1997) *Biochim. Biophys. Acta 1318*, 11–51.
4. Nelson, N. (1989) *J. Bioenerg. Biomembr. 21*, 553–571.
5. Bowman, B. J., and Bowman, E. J. (1997) in *The Mycota III. Biochemistry And Molecular Biology* (Brambl and Marzluf, Eds.) pp 57–83.
6. Tomashek, J. J., Graham, L. A., Hutchins, M. U., Stevens, T. H., and Klionsky, D. J. (1997) *J. Biol. Chem. 272*, 26787–26793.
7. Dschida, W. J., and Bowman, B. J. (1992) *J. Biol. Chem. 267*, 18783–18789.
8. Harvey, W. R. (1992) *J. Exp. Biol. 172*, 1–17.
9. Abrahams, J. P., Leslie, A. G. W., Lutter, R., and Walker, J. E. (1994) *Nature 370*, 621–628.
10. Bianchet, M. A., Hullihen, J., Pedersen, P. L., and Amzel, M. L. (1998) *Proc. Natl. Acad. Sci. U.S.A. 95*, 11065–11070.
11. Koch, M. H. J., and Bordas, J. (1983) *Nucl. Instrum. Methods 208*, 461–469.
12. Boulin, C., Kempf, R., Koch, M. H. J., and McLaughlin, S. M. (1986) *Nucl. Instrum. Methods A249*, 399–407.
13. Boulin, C. J., Kempf, R., Gabriel, A., and Koch, M. H. J. (1988) *Nucl. Instrum. Methods A269*, 312–320.
14. Gabriel, A., and Dauvergne, F. (1982) *Nucl. Instrum. Methods 201*, 223–224.
15. Svergun, D. I. (1993) *J. Appl. Crystallogr. 26*, 258–267.
16. Svergun, D. I., Semenyuk, A. V., and Feigin, L. A. (1988) *Acta Crystallogr., Sect. A 44*, 244–250.
17. Svergun, D. I. (1992) *J. Appl. Crystallogr. 25*, 495–503.
18. Feigin, L. A., and Svergun, D. I. (1987) Plenum Press, New York.
19. Svergun, D. I., and Stuhrmann, H. B. (1991) *Acta Crystallogr., Sect. A 47*, 736–744.
20. Svergun, D. I., Volkov, V. V., Kozin, M. B., and Stuhrmann, H. B. (1996) *Acta Crystallogr., Sect. A 52*, 419–426.
21. Svergun, D. I., Volkov, V. V., Kozin, M. B., Stuhrmann, H. B., Barberato, C., and Koch, M. H. J. (1997) *J. Appl. Crystallogr. 30*, 798–802.
22. Stuhrmann, H. B. (1970) *Z. Phys. Chem. 72*, 177–198.
23. Shirakihara, Y., Leslie, A. G. W., Abrahams, J. P., Walker, J. E., Ueda, T., Sekimoto, Y., Kambara, M., Saika, K., Kagawa, Y., and Yoshida, M. (1997) *Structure 5*, 825–836.
24. Gräf, R., Harvey, W. R., and Wieczorek, H. (1996) *J. Biol. Chem. 271*, 20908–20913.
25. Wieczorek, H., Cioffi, M., Klein, U., Harvey, W. R., Schweikl, H., and Wolfersberger, M. G. (1990) *Methods. Enzymol. 192*, 608–616.
26. Grüber, G., Hausrath, A., Sagermann, M., and Capaldi, R. A. (1997) *FEBS Lett. 410*, 165–168.
27. Dulley, J. R., and Gieve, P. (1975) *Anal. Biochem. 64*, 136–147.
28. Fiske, C. H., and Subarow, Y. (1925) *J. Biol. Chem. 271*, 32623–32628.
29. Arnold, A., Wolf, H. U., Ackermann, B. P., and Bader, H. (1976) *Anal. Biochem. 71*, 209–213.
30. Sumner, J. P., Dow, J. A. T., Earley, F. G. P., Klein, U., Jäger, D., and Wieczorek, H. (1995) *J. Biol. Chem. 270*, 5649–5653.
31. Merzendorfer, H., Gräf, R., Huss, M., Harvey, W. R., and Wieczorek, H. (1997) *FEBS Lett. 411*, 239–244.
32. Ho, M. N., Hirata, R., Umemoto, N., Ohya, Y., Takatsuki, A., Stevens, T. H., and Anraku, Y. (1993) *J. Biol. Chem. 268*, 18286–18292.
33. Xie, X. S., Crider, B. P., Ma, Y. M., and Stone, D. K. (1994) *J. Biol. Chem. 269*, 25809–25815.
34. Svergun, D. I., Volkov, V. V., Kozin, M. B., Stuhrmann, H. B., Barberato, C., and Koch, M. H. J. (1997) *J. Appl. Crystallogr. 30*, 798–802.
35. Nelson, H., Mandiyan, S., and Nelson, N. (1995) *Proc. Natl. Acad. Sci. U.S.A. 92* (2), 497–501.
36. Bowman, E. J., Steinhardt, A., and Bowman, B. J. (1995) *Biochim. Biophys. Acta 1237*, 95–98.
37. Hunt, I. E., and Bowman, B. J. (1997) *J. Bioenerg. Biomembr. 29*, 533–540.
38. Lepier, A., Gräf, R., Azuma, M., Merzendorfer, H., Harvey, W. R., and Wieczorek, H. (1996) *J. Biol. Chem. 271*, 8502–8508.

39. Gräf, R., Lepier, A., Harvey, W. R., and Wieczorek, H. (1994) *J. Biol. Chem. 269*, 3767−3774.

40. Boekema, E. J., Ubbink-Kok, T., Lolkema, J. S., Brisson, A., and Konings, W. N. (1997) *Proc. Natl. Acad. Sci. U.S.A. 94*, 14291−14293.

41. Svergun, D. I., Aldag, I., Sieck, T., Altendorf, K., Koch, M. H. J., Kane, D. J., Kozin, M. B., and Grüber, G. (1998) *Biophys. J. 75*, 2212−2219.

42. Cross, R. L., and Duncan, T. M. (1996) *J. Bioenerg. Biomembr. 28*, 403−408.

43. Junge, W., Lill, H., and Engelbrecht, S. (1997) *Trends Biochem. Sci. 22*, 420−423.

44. Fillingame, R. H. (1997) *J. Exp. Biol. 200*, 217−224, 1997.

45. Kinosita, K., Jr., Yasuda, R., Noji, H., Ishiwata, S., and Yoshida, M. (1998) *Cell 93*, 21−24.

46. Capaldi, R. A., Aggeler, R., Wilkens, S., and Grüber, G. (1996) *J. Bioenerg. Biomembr. 28*, 397−401.

47. Svergun, D. I., Barberato, C., Koch, M. H. J., Fetler, L., and Vachette, P. (1997) *Proteins 27*, 110−117.

48. Kozin, M. B., Volkov, V. V., and Svergun, D. I. (1997) *J. Appl. Crystallogr. 30*, 811−815.

BI982367A